

Theory of the conductivity and giant magnetoresistance in magnetic multilayers

Hideo Hasegawa

Department of Physics, Tokyo Gakuai University, Koganei, Tokyo 184, Japan
(Received 20 October 1992; revised manuscript received 1 February 1993)

A simple, analytic expression is derived for the conductivity of thin films with the use of the coherent-potential approximation. With the use of our conductivity formula, the giant magnetoresistance in multilayers consisting of magnetic and nonmagnetic layers, is discussed based on a numerical calculation for seven-layer Fe/Cr films and a semiphenomenological analysis for a simple model.

I. INTRODUCTION

Since the discovery of giant magnetoresistance (GMR) in Fe/Cr multilayers,¹ related phenomena have been intensively investigated for many multilayers consisting of magnetic and nonmagnetic layers.² It has been found that the GMR in multilayers arise from the reorientation of moments on magnetic layers due to an applied magnetic field. The antiferromagnetically coupled magnetic moments on successive magnetic layers align ferromagnetically by the applied field, which yields a significant reduction in the resistivity. The theoretical understanding of the GMR has been made by the semiclassical approach^{3,4} using the Boltzman equation or the microscopic method⁵⁻⁷ starting from the Kubo formula. Quite recently, Okiji *et al.*⁷ employed the transport theory in the coherent potential approximation (CPA).^{8,9} Assuming that currents flow along the x axis in the plane of a multilayer, they numerically calculated the ground-state parallel conductivity of the multilayer given by

$$\sigma = (e/\hbar)^2 \sum_{k_{\parallel}} (\partial \varepsilon_k / \partial k_x)^2 \times \sum_{nm} \text{Im} G_{nm}(k_{\parallel}, \mu) \text{Im} G_{mn}(k_{\parallel}, \mu), \quad (1)$$

where k_{\parallel} is the two-dimensional surface wave vector, ε_k the dispersion, and G_{nm} denotes the interlayer Green function between the n th and m th layers at the Fermi level μ . They calculated the conductivities when moments on adjacent magnetic layers align ferromagnetically and antiferromagnetically, from which the magnetoresistance was calculated. Their calculation demonstrates that the study on the magnetoresistance of multilayers using Eq. (1) is very useful. The actual numerical computation is, however, rather laborious because it requires many sampling k_{\parallel} points (more than 10 000) in the reduced surface Brillouin zone. Furthermore, the numerical calculation cannot well explain the physical mechanism yielding the GMR. One of the purposes of the present study is to derive a simpler, but physically more transparent, analytic expression for the conductivity based on Eq. (1). The other purpose is to investigate the mechanism of the GMR by using our formula for the

conductivity.

The paper is organized as follows: In Sec. II, the expression for the conductivity is derived by using the CPA. With the use of our conductivity formula, the GMR is discussed in Sec. III, with model calculations based on a numerical study for a seven-layer Fe/Cr film and a semiphenomenological study for a simple model. Section IV is devoted to conclusion and supplementary discussion.

II. FORMULATION FOR CONDUCTIVITY OF FILMS

In order to rewrite Eq. (1), it is necessary to get the explicit form of the Green function, G_{nm} . We adopt an N_f -layer thin film consisting of magnetic A and nonmagnetic B atoms with the simple-cubic (001) interface. The layer parallel to the interface is assigned by the index n ($= 1 - N_f$). We introduce the randomness at the interface and/or throughout the layer (bulk), allowing the atomic potentials to be random. The system is described by the single-band Hamiltonian with the nearest-neighbor hopping t as

$$H = \sum_s \sum_j \varepsilon_{js} c_{js}^{\dagger} c_{js} + t \sum_s \sum_{jl} c_{js}^{\dagger} c_{ls}, \quad (2)$$

where c_{js} is an annihilation operator of an electron with spin s ($= \uparrow, \downarrow$) on the lattice site j . The s -spin atomic potential on the layer n , ε_{ns} , is assumed to be ε_{ns}^A and ε_{ns}^B with the probabilities x_n and y_n ($= 1 - x_n$) when the lattice site j is occupied by the A and B atoms, respectively. The introduced randomness is treated by the CPA.⁹ The effective Hamiltonian is expressed in the Bloch-Wannier representation as

$$H_{\text{eff}} = \sum_s \sum_{k_{\parallel}} \sum_{nm} [(\Sigma_{ns} + \varepsilon_{k_{\parallel}}) \delta_{n,m} + t(\delta_{m,n+1} + \delta_{m,n-1})] c_{k_{\parallel}ns}^{\dagger} c_{k_{\parallel}ms}, \quad (3)$$

where $c_{k_{\parallel}ns}$ is the Fourier transform of c_{js} , and Σ_{ns} is the layer- and spin-dependent coherent potential determined by

$$\langle (\Sigma_{ns} - \varepsilon_{ns}) / [1 - (\Sigma_{ns} - \varepsilon_{ns}) F_{ns}(z)] \rangle_n = 0, \quad (4)$$

with

$$F_{ns}(z) = \sum_{k_{\parallel}} G_{nns}(k_{\parallel}, z). \quad (5)$$

Here the angular brackets $\langle \rangle_n$ denotes the configuration average over the random ε_{ns} .

The Green function G_{nm} of the effective Hamiltonian is given by

$$G_{nm}(k_{\parallel}, z) = \langle k_{\parallel}n | (z - H_{\text{eff}})^{-1} | k_{\parallel}m \rangle \quad (6)$$

$$= C_{mn}/D, \quad (7)$$

where $|k_{\parallel}m\rangle$ is the eigenstate with momentum k_{\parallel} on layer m , and C_{mn} is the cofactor of the mn element of determinant of the energy matrix: $D = \det|z - H_{\text{eff}}|$, the spin index being suppressed for a while. When D_i ($i = 1 - N_f$) is the root of $D = 0$, Eq. (7) is rewritten as

$$G_{nm}(k_{\parallel}, z) = \prod_i C_{mn}/(z - \varepsilon_{k_{\parallel}} - D_i) \quad (8)$$

$$= \sum_i A_{nm}^{(i)}/(z - \varepsilon_{k_{\parallel}} - D_i), \quad (9)$$

with

$$A_{nm}^{(i)} = \prod_{j(\neq i)} C_{mn}(D_j)/(D_j - D_i). \quad (10)$$

In Eq. (10) $C_{mn}(D_j)$ is the cofactor of the determinant in which we set $z - \varepsilon_{k_{\parallel}} = D_j$. We assume the absence of the degeneracy in D_i for a simplicity of our discussion. We expect that D_i is nearly equal to Σ_i given by

$$D_i \simeq \Sigma_i = \Lambda_i - i\Delta_i, \quad (11)$$

where $\Lambda_i = \text{Re}\Sigma_i$ and $\Delta_i = |\text{Im}\Sigma_i|$. Substituting the imaginary part of the Green function given by Eqs. (9)–(11) to Eq. (1), and, introducing the function

$$\nu^0(\omega) = \sum_{k_{\parallel}} (\partial\varepsilon_k/\partial k_x)^2 \delta(\omega - \varepsilon_{k_{\parallel}}), \quad (12)$$

we transform the summation over $\varepsilon_{k_{\parallel}}$ in Eq. (1) to the integral over energy ω . Then we define a complex function given by

$$\Phi(\omega) = \int d\omega' \nu^0(\omega')/(\omega - \omega'), \quad (13)$$

to perform the contour integral in the *complex- ω* plane. Since the general expression for the conductivity is rather cumbersome, we confine in this paper our discussion to the weak-scattering case.

In the weak-scattering limit, the imaginary part of the Green function is expressed by

$$\text{Im}G_{nm}(k_{\parallel}, z) = \sum_i A_{nm}^{(i)} \Delta_i / [(z - \varepsilon_{k_{\parallel}} - \Lambda_i)^2 + \Delta_i^2], \quad (14)$$

where $A_{nm}^{(i)}$ is given by Eq. (10) but with $D_i = \Lambda_i$. Substituting Eq. (14) for Eq. (1), and interchanging variables nm with ij , we get the conductivity *per layer* for the current parallel to film layers, given by

$$\sigma = (e/\hbar)^2 N_f^{-1} \sum_{nm} a_{nm} X_{nm}, \quad (15)$$

where

$$a_{nm} = \sum_{ij} A_{ij}^{(n)} A_{ji}^{(m)}, \quad (16)$$

$$X_{nm} = \int \frac{d\omega \nu^0(\omega + \mu) \Delta_n \Delta_m}{[(\omega + \Lambda_n)^2 + \Delta_n^2][(\omega + \Lambda_m)^2 + \Delta_m^2]}. \quad (17)$$

After extracting residues in the complex- ω plane to evaluate Eq. (17), we finally obtain the expression for the parallel conductivity given by

$$\sigma = N_f^{-1} \sum_s \sum_n \sigma_{ns}, \quad (18)$$

where

$$\sigma_{ns} = (e/\hbar)^2 \pi \nu_s \sum_m \frac{a_{nms} \tau_{nms}}{(\Delta_{ns} + \Delta_{ms})}, \quad (19)$$

$$\nu_s = (-1/\pi) \text{Im}\Phi(\mu_s + i0), \quad (20)$$

$$\tau_{nms} = \delta_{nm} + (1 - \delta_{nm}) \times \left(\frac{(\Delta_{ns} + \Delta_{ms})^2}{[(\Lambda_{ns} - \Lambda_{ms})^2 + (\Delta_{ns} + \Delta_{ms})^2]} \right). \quad (21)$$

The spin index s is recovered in Eqs. (18)–(21), where meanings of the spin dependence in various quantities are obvious.

The analytical expression given by Eqs. (18)–(21) has clear physical meaning. An electron with spin s successively propagates from a site on layer n to a site on layer m . In this process the electron is scattered with the strength proportional to Δ_{ns} and Δ_{ms} . Total conductivity is given as a sum of such processes with the weight of $a_{nms} \tau_{nms}$. The coefficient a_{nms} and the function ν_s are specified by the electronic structure of the film. The factor τ_{nms} plays a role of a *valve* in the transmission process between the layers n and m . This is easily seen in the expression of τ_{nms} for $n \neq m$ (see Fig. 1):

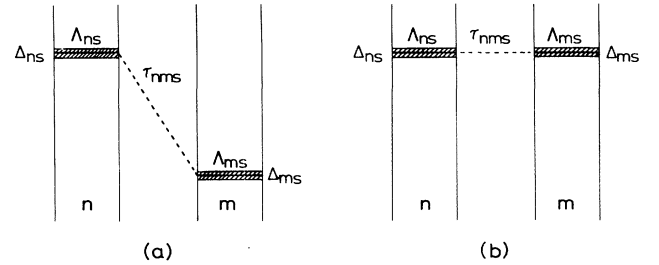


FIG. 1. Schematic representation of the valve effect showing the cases of (a) $\tau_{nms} \simeq 0$ for $|\Lambda_{ns} - \Lambda_{ms}| \gg (\Delta_{ns} + \Delta_{ms})$ and (b) $\tau_{nms} \simeq 1$ for $|\Lambda_{ns} - \Lambda_{ms}| \ll (\Delta_{ns} + \Delta_{ms})$. The center hatched bands and their width denote Λ_{ns} and Δ_{ns} , respectively.

$$\begin{aligned} \tau_{nms} &\simeq 0 && \text{for } |\Lambda_{ns} - \Lambda_{ms}| \gg (\Delta_{ns} + \Delta_{ms}), && (22) \\ &\simeq 1 && \text{for } |\Lambda_{ns} - \Lambda_{ms}| \ll (\Delta_{ns} + \Delta_{ms}). && (23) \end{aligned}$$

Depending on the value of $|\Lambda_{ns} - \Lambda_{ms}|$, τ_{nms} changes its value from 0 to 1. In the case given by Eq. (22), the system can be regarded as a collection of independent networks with the parallel connection. The case given by Eq. (23) is realized when moments on successive magnetic layer are parallel, as will be discussed shortly.

When the system is nonmagnetic and homogeneous (bulk), $\Delta_{ns} = \Delta$ ($= \text{const}$) and $\Lambda_{ns} = \Lambda$ ($= \text{const}$), Eqs. (18)–(21) yield the relations

$$\sigma = (e/\hbar)^2 (\pi\nu)/\Delta, \quad (24)$$

$$\sum_{nm} a_{nm} = N_f. \quad (25)$$

Equation (24) agrees with the result for bulk alloys in the Born approximation.⁸

III. MODEL CALCULATIONS

A. Numerical study

First we show some numerical examples by applying our formalism to a seven-layer Fe/Cr film with the simple-cubic (001) interface. We assumed the distribution of Fe concentration on layer n , x_n , as $x_1 = x_7 = 0.95$, $x_2 = x_6 = 0.90$, $x_3 = x_5 = 0.10$ and $x_4 = 0.05$, as depicted in Fig. 2(a). The randomness is introduced mainly

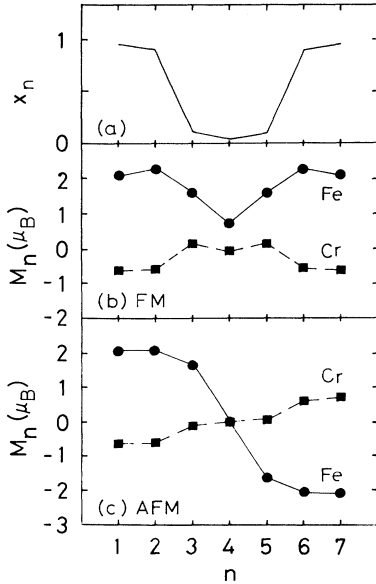


FIG. 2. (a) The assumed Fe concentration on the n th layer x_n in seven-layer Fe/Cr films with the simple-cubic (001) interface. Calculated magnetic moments are on the n th layer, M_n (μ_B), at Fe (solid curves), and Cr sites (dashed curves) in the (b) ferromagnetic (FM) and (c) antiferromagnetic (AFM) solutions.

at the Fe/Cr interfaces. Actual calculations were performed for a nine-layer film, each edge of the seven-layer film was capped by a pure Fe layer. The calculated results in the inner seven-layer film were employed for the conductivity calculation in order to reduce the edge effect. On Fe sites we introduced the electron-electron interaction, U^{Fe} , which is treated in the Hartree-Fock approximation. We adopted the parameters of $\varepsilon^{\text{Fe}} - \varepsilon^{\text{Cr}} = -1.47$, $U^{\text{Fe}} = 1.50$ and $U^{\text{Cr}} = 0$ in units of W , a half of the total width of the simple-cubic bulk band. The magnetic moment, M_n^λ , the number of electrons, N_n^λ ($\lambda = \text{Fe, Cr}$), and the coherent potential of each layer were self-consistently determined in the CPA. Details of the adopted calculation method were discussed elsewhere.¹⁰

As in previous calculations for Fe/Cr multilayers,^{10,11} we obtained both the ferromagnetic (FM) and antiferromagnetic (AFM) solutions, whose moment distributions are shown in Figs. 2(b) and 2(c), respectively.¹² The real parts of the layer- and spin-dependent coherent potentials, Λ_{ns} , which are self-consistently determined for the FM and AFM solutions, are shown in Figs. 3(a) and 3(b), respectively. The exchange splittings, $|\Lambda_{n\uparrow} - \Lambda_{n\downarrow}|$, in Fe layers are about 0.6 in units of W , whereas those in Cr layers are fairly small. Figures 4(a) and 4(b) show the imaginary parts of the coherent potentials, Δ_{ns} , in the FM and AFM solutions, respectively. The behaviors of the calculated Λ_{ns} and Δ_{ns} are easily understood from the following expressions valid in the Born approximation:^{8,9}

$$\Lambda_{ns} = x_n \varepsilon_{ns}^{\text{Fe}} + y_n \varepsilon_{ns}^{\text{Cr}}, \quad (26)$$

$$\Delta_{ns} = \pi \rho_{ns} x_n y_n (\varepsilon_{ns}^{\text{Fe}} - \varepsilon_{ns}^{\text{Cr}})^2, \quad (27)$$

where $\varepsilon_{ns}^\lambda = \varepsilon^\lambda + (U^\lambda/2)N_n^\lambda - s(U^\lambda/2)M_n^\lambda$ ($\lambda = \text{Fe, Cr}$), and ρ_{ns} is the s -spin local density of states on the layer n . In the FM solution, $\Delta_{n\uparrow}$ is much larger than $\Delta_{n\downarrow}$, which arises from the fact that $|\varepsilon_{n\uparrow}^{\text{Fe}} - \varepsilon_{n\uparrow}^{\text{Cr}}| \gg |\varepsilon_{n\downarrow}^{\text{Fe}} - \varepsilon_{n\downarrow}^{\text{Cr}}|$ [see Eq. (27)].⁶ The similar situation is realized also in the AFM solution, where $\Delta_{n\uparrow} \gg \Delta_{n\downarrow}$ at $n = 1-3$ and $\Delta_{n\downarrow} \gg \Delta_{n\uparrow}$ at $n = 5-7$. We note that the scattering strengths

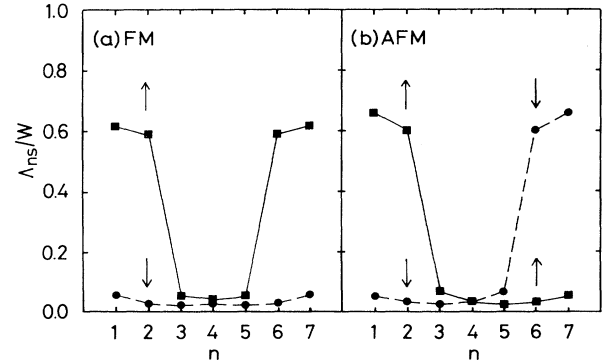


FIG. 3. The real parts of the coherent potentials Λ_{ns} for up-spin (solid curves) and down-spin (dashed curves) electrons in the (a) FM and (b) AFM solutions in units of W , half of the total width of the simple-cubic bulk band.

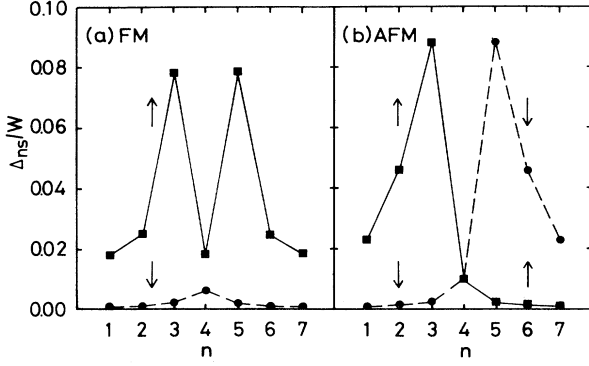


FIG. 4. The imaginary part of the coherent potential Δ_{ns} for up-spin (solid curves) and down-spin (dashed curves) electrons in the (a) FM and (b) AFM solutions in units of W .

at the Cr interface ($n = 3, 5$) are most significant both in the FM and AFM solutions.

With the use of Λ_{ns} and Δ_{ns} thus determined, the film conductivity was calculated from Eqs. (18)–(21). We assumed that a_{nms} and ν_s are constants because they are considered to be important for our qualitative discussion (see below). The calculated layer- and spin-dependent conductivities, σ_{ns} , for the FM and AFM states are shown by solid curves in Figs. 5(a) and 5(b), respectively, where squares (circles) denote the up-spin (down-spin) conductivity. In the FM state, the down-spin conductivity is much higher than the up-spin one because $\Delta_{n\uparrow} \gg \Delta_{n\downarrow}$ (Fig. 4).^{6,7} Our result of σ_{ns} is consistent with what Okiji *et al.*⁷ calculated with the *s-d* model using Eq. (1). This justifies to some extent the approximation adopted in our numerical calculation for the Fe/Cr thin film. The layer-dependent (spin-summed) conductivity, $\sigma_n = \sum_s \sigma_{ns}$, in the FM and AFM states are

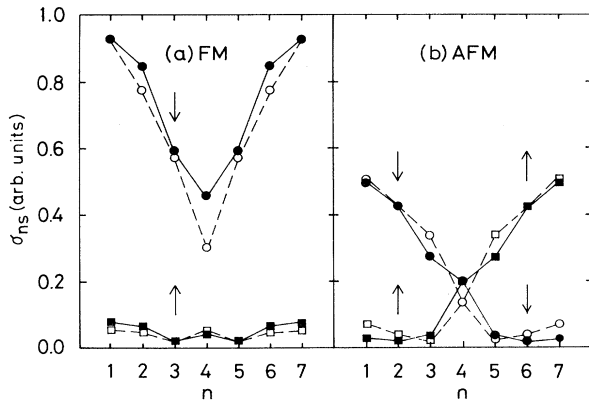


FIG. 5. The layer- and spin-dependent conductivity σ_{ns} in the (a) FM and (b) AFM configurations; squares (circles) expressing the up-spin (down-spin) contribution. Solid curves show the results calculated by using Eqs. (19)–(21). Dashed curves are those with setting $\tau_{nms} = 1$ in Eq. (21), which corresponds to the neglect of the valve effect. Results shown by solid and dashed curves are normalized to coincide at σ_{ns} for $n = 1$ and $s = \downarrow$ (see text).

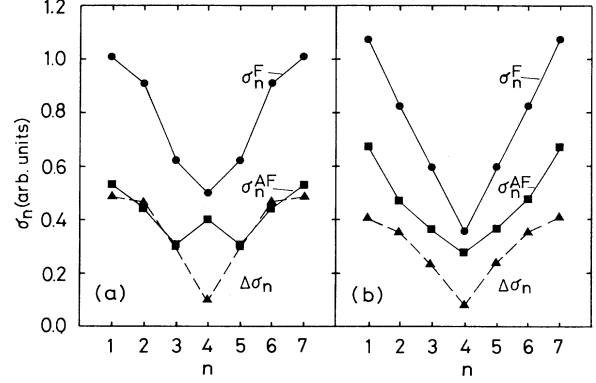


FIG. 6. (a) The layer-dependent (spin-summed) conductivity in the FM (σ_n^{FM}) and AFM (σ_n^{AFM}) and the difference: $\Delta\sigma_n = \sigma_n^{\text{FM}} - \sigma_n^{\text{AFM}}$ (in the normalized units same as in Fig. 5). (b) The same as (a) but setting $\tau_{nms} = 1$ in Eq. (21) (see text).

shown by solid curves in Fig. 6(a), where their difference, $\Delta\sigma_n = \sigma_n^{\text{FM}} - \sigma_n^{\text{AFM}}$, are plotted by the dashed curve. We note that the conductivity contributions from Fe layers and interface layers are much reduced when moment configuration changes from FM to AFM state. The MR ratio defined by

$$\Delta R/R^{\text{FM}} = (R^{\text{AFM}} - R^{\text{FM}})/R^{\text{FM}} = \Delta\sigma/\sigma^{\text{AFM}}, \quad (28)$$

is $\Delta R/R^{\text{FM}} = 0.88$ in our Fe/Cr film, where R^n is the resistivity in the η ($=\text{AFM, FM}$) configuration.

In order to investigate the valve effect of τ_{nms} given by Eq. (21), we repeated the conductivity calculation by setting $\tau_{nms} = 1$, which corresponds to an assumption: $\Lambda_{ns} = \text{const}$. The up-spin and down-spin conductivities calculated for the FM and AFM states are shown by dashed curves in Figs. 5(a) and 5(b), respectively. The layer-dependent conductivity in the FM and AFM states are shown by solid curves in Fig. 6(b), where the dashed curve denotes the difference $\Delta\sigma_n$. When setting $\tau_{nms} = 1$, the electron transmission between layers n and m is increased, and the total conductivity, particularly of the AFM state, is increased. Then the MR ratio reduces to $\Delta R/R^{\text{FM}} = 0.67$, about a 25% reduction from its original value. This shows that the factor of τ_{nms} might play an important role in the GMR.

B. Semiphenomenological study

Next we discuss the GMR by phenomenologically using the expression given Eqs. (18)–(21). We adopt the system consisting of magnetic (M_1, M_2) and nonmagnetic (N_1, N_2) layers (see Fig. 7). The thickness of each magnetic (nonmagnetic) layer is M (N). Bulk scatterings are assumed to be important in these layers, while in the Sec. III A the interface scatterings were assumed to be dominant. When moments on the magnetic layers are in the AFM configuration, as shown in Fig. 7(a), the real and imaginary parts of the coherent potentials are given by¹³

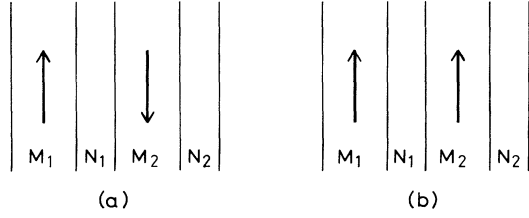


FIG. 7. The adopted film consisting of magnetic (M_1 and M_2) and nonmagnetic (N_1 and N_2) layers, their thickness being M and N , respectively. The moments on the magnetic layers align in the (a) AFM and (b) FM configurations.

$$\Lambda_{ns}^{\text{AFM}} - i\Delta_{ns}^{\text{AFM}} = \Lambda_s - i\Delta_s \quad \text{for } n \in M_1, \quad (29)$$

$$= \Lambda_{-s} - i\Delta_{-s} \quad \text{for } n \in M_2, \quad (30)$$

$$= \Lambda_0 - i\Delta_0 \quad \text{for } n \in N_1, N_2. \quad (31)$$

The s -spin contribution to the conductivity is classified into five categories depending on whether n and m are in magnetic or nonmagnetic layers. It is given by

$$\begin{aligned} \sigma_s^{\text{AFM}} = & \frac{2c_{MM}^{\text{AFM}}}{(\Delta_s + \Delta_{-s})} + \frac{c_{NN}^{\text{AFM}}}{\Delta_0} \\ & + 4c_{MN}^{\text{AFM}} \left(\frac{1}{\Delta_s + \Delta_0} + \frac{1}{\Delta_{-s} + \Delta_0} \right) \\ & + d_M^{\text{AFM}} \left(\frac{1}{2\Delta_s} + \frac{1}{2\Delta_{-s}} \right) + \frac{d_N^{\text{AFM}}}{\Delta_0}, \end{aligned} \quad (32)$$

where

$$c_{MM}^{\text{AFM}} = N_f^{-1} (e/\hbar)^2 \pi \nu \sum_{n \in M_1} \sum_{m \in M_2} a_{nm} \tau_{nm}, \quad (33)$$

$$d_M^{\text{AFM}} = N_f^{-1} (e/\hbar)^2 \pi \nu \sum_{n \in M_1} \sum_{m \in M_1} a_{nm} \tau_{nm}, \quad (34)$$

and c_{NN}^{AFM} , c_{MN}^{AFM} , and d_N^{AFM} are given by similar expressions, the spin dependence in a_{nms} and τ_{nms} being neglected. In Eq. (32), subscripts MM , NN , and MN denote the contributions from the *interlayer* scatterings between magnetic layers, between nonmagnetic layers, and between magnetic and nonmagnetic layers, respec-

tively. On the other hand, the single subscript $M(N)$ expresses the contribution from the *intralayer* scatterings within magnetic (nonmagnetic) layers.

In the FM configuration, as shown in Fig. 7(b), the real and imaginary parts of the coherent potentials are given by¹³

$$\Lambda_{ns}^{\text{FM}} - i\Delta_{ns}^{\text{FM}} = \Lambda_s - i\Delta_s \quad \text{for } n \in M_1, M_2, \quad (35)$$

$$= \Lambda_0 - i\Delta_0 \quad \text{for } n \in N_1, N_2. \quad (36)$$

The s -spin contribution to the conductivity becomes

$$\sigma_s^{\text{FM}} = \frac{c_{MM}^{\text{FM}}}{\Delta_s} + \frac{c_{NN}^{\text{FM}}}{\Delta_0} + \frac{8c_{MN}^{\text{FM}}}{\Delta_s + \Delta_0} + \frac{d_M^{\text{FM}}}{\Delta_s} + \frac{d_N^{\text{FM}}}{\Delta_0}. \quad (37)$$

The total conductivity for ferromagnetic and antiferromagnetic configurations are obtained by summing both the up-spin and down-spin contributions [Eq. (18)].

The difference between the total conductivities in the FM (σ^{FM}) and AFM (σ^{AFM}) configurations is given by

$$\begin{aligned} \Delta\sigma = & \sigma^{\text{FM}} - \sigma^{\text{AFM}} \\ = & c_{MM}^{\text{FM}} \left(\frac{1}{\Delta_\uparrow} + \frac{1}{\Delta_\downarrow} \right) - 4c_{MM}^{\text{AFM}} \left(\frac{1}{\Delta_\uparrow + \Delta_\downarrow} \right), \quad (38) \\ = & \frac{c_{MM}}{\Delta_0 \alpha \beta (\alpha + \beta)} [(\alpha - \beta)^2 + \gamma(\alpha^2 + 6\alpha\beta + \beta^2)], \end{aligned} \quad (39)$$

where

$$\alpha = \Delta_\uparrow / \Delta_0, \quad \beta = \Delta_\downarrow / \Delta_0, \quad \gamma = \delta c_{MM} / c_{MM}, \quad (40)$$

$$c_{MM} = (c_{MM}^{\text{FM}} + c_{MM}^{\text{AFM}}) / 2, \quad \delta c_{MM} = (c_{MM}^{\text{FM}} - c_{MM}^{\text{AFM}}) / 2, \quad (41)$$

the configuration dependence of the coefficients being included only in c_{MM} . Equation (38) shows that the GMR arises mainly from the conductivity contribution from interlayer scatterings between the magnetic layers M_1 and M_2 because other contributions in Eqs. (32) and (37) are canceled out in calculating the difference $\Delta\sigma$.

The MR ratio is given, by using Eqs. (28), (32), (37), and (38), as

$$\frac{\Delta R}{R^{\text{FM}}} = \frac{\Delta R^{(1)}}{R^{\text{FM}}} + \frac{\Delta R^{(2)}}{R^{\text{FM}}}, \quad (42)$$

with

$$\frac{\Delta R^{(1)}}{R^{\text{FM}}} = \frac{(\alpha - \beta)^2}{4\alpha\beta \left[1 - \gamma + g_0 \frac{(\alpha + \beta)^2}{\alpha\beta} + g_1 \left(\frac{N}{M} \right) (\alpha + \beta) \left(\frac{1}{\alpha + 1} + \frac{1}{\beta + 1} \right) + g_2 \left(\frac{N}{M} \right)^2 (\alpha + \beta) \right]}, \quad (43)$$

$$\frac{\Delta R^{(2)}}{R^{\text{FM}}} = \frac{\gamma(\alpha^2 + 6\alpha\beta + \beta^2)}{4\alpha\beta \left[1 - \gamma + g_0 \frac{(\alpha + \beta)^2}{\alpha\beta} + g_1 \left(\frac{N}{M} \right) (\alpha + \beta) \left(\frac{1}{\alpha + 1} + \frac{1}{\beta + 1} \right) + g_2 \left(\frac{N}{M} \right)^2 (\alpha + \beta) \right]}, \quad (44)$$

In Eqs. (43) and (44), g_0 , g_1 , and g_2 are defined by

$$\frac{d_M}{4c_{MM}} = g_0, \quad \frac{2c_{MN}}{c_{MM}} = g_1 \left(\frac{N}{M} \right), \quad (45)$$

$$\left(\frac{c_{NN} + d_N}{2c_{MM}} \right) = g_2 \left(\frac{N}{M} \right)^2,$$

which come from the following relations:

$$c_{MN} \propto MN, \quad c_{NN} \propto d_N \propto N^2, \quad (46)$$

$$c_{MM} \propto d_M \propto M^2.$$

The first term of Eq. (42) expresses the “short-circuit” effect: The total conductivity of the FM state is generally larger than that of the AFM state because the more-conductive \uparrow - (or \downarrow -) spin channel in the FM state short-circuits the circuit. This mechanism was discussed previously in Refs. 3–7. Using a resistor network model based on the phenomenological approach, Edwards, Mathon, and Muniz⁴ obtained the MR ratio given by

$$\frac{\Delta R}{R^{\text{FM}}} = \frac{(\alpha - \beta)^2}{4\alpha\beta \left[1 + \left(\frac{N}{M} \right) [(\alpha + \beta)/\alpha\beta] + \left(\frac{N}{M} \right)^2 (1/\alpha\beta) \right]}, \quad (47)$$

which has a structure similar to our Eq. (43). If we set $g_0 = g_1 = g_2 = \gamma = 0$ in Eq. (43), the MR ratio becomes

$$\Delta R/R^{\text{FM}} = (\alpha - \beta)^2/4\alpha\beta, \quad (48)$$

which agrees with the result obtained by Levy and co-workers⁵ and Inoue, Oguri, and Maekawa.⁶

On the other hand, the second term in Eq. (42) arises from the “valve” effect of τ_{nms} as discussed before [see Eqs. (22) and (23)]. In the FM state, τ_{nms} between the M_1 and M_2 layers becomes large because Λ_{ns} on M_1 layer is nearly equal to Λ_{ms} on M_2 layers. On the other hand, this is not the case in the AFM state in which Λ_{ns} on M_1 layer is much different from Λ_{ms} on M_2 layer. This leads to $c_{MM}^{\text{FM}} \geq c_{MM}^{\text{AFM}}$, and then $\gamma \geq 0$ in Eqs. (40) and (41). We note from Eq. (39) that $\Delta\sigma \geq 0$ (i.e., $\sigma^{\text{FM}} \geq \sigma^{\text{AFM}}$) because α , β , and γ are positive definite.

Both the short-circuit and valve effects are the origin of the GMR. The short-circuit effect always exists as far as $\alpha \neq \beta$ even if $\gamma = 0$. On the contrary, the valve effect exists when $\gamma \neq 0$ even if $\alpha = \beta$. It should be pointed out that the valve effect also works to enhance the short-circuit effect because of γ in the denominator of Eq. (43).

IV. CONCLUSION AND DISCUSSION

To summarize, we have derived the simple, analytic expression for the film conductivity with the use of CPA,^{8,9} treating the interface and bulk scatterings on the same footing. Although our discussion has been made for thin films, the essential result obtained in this study is expected to be valid for any multilayers. We have discussed the short-circuit and valve effects, which are the origin of the GMR. These effects have been investigated by numerical calculations for seven-layer Fe/Cr films and a semiphenomenological analysis. The GMR is shown to arise from conductivity contributions from the *interlayer* scatterings between the successive magnetic layers which are much reduced when the FM configuration is changed to the AFM.

Our conductivity formulas are expected to have a wide applicability. We may make a detailed calculation taking into account the electronic structure of films. It is also possible to use our expression phenomenologically, just as we have made in Sec. III B. One of the advantage of the CPA theory is that it preserves the Ward identity.⁸ The one-body physical quantity like magnetic moments and the two-body quantity such as the conductivity and susceptibility can be calculated in a consistent way. The second advantage of the CPA is that we can perform *realistic* calculations for multilayers including randomness at the interface¹¹ and/or in bulk.

In this paper, the imaginary part of the coherent potential arises from the randomness in film layers. According to the recent theories on magnetism for finite-temperature properties,¹⁴ the effect of spin fluctuations can be taken into account by regarding them as static random potentials (so-called alloy-analogy approximation).^{15,16} By combining our result with the finite-temperature band theory,¹⁵ we may discuss the magnetoresistance of multilayers at finite temperatures. Such a calculation will be reported separately.¹⁷

ACKNOWLEDGMENTS

The author wishes to express his sincere thanks to Professor S. Maekawa and Professor J. Inoue for valuable discussions. This work was partly supported by a Grant-in-Aid for Scientific Research on Priority Areas from the Japanese Ministry of Education, Science and Culture.

¹M. N. Baibich, J. M. Broto, A. Fert, N. Nuyuen Van Dau, F. Petroff, P. Eitenne, G. Creuzet, A. Friedrich, and J. Chazelas, *Phys. Rev. Lett.* **61**, 2472 (1988); G. Binash, P. Grünberg, F. Saurenbach, and W. Zinn, *Phys. Rev. B* **39**, 4828 (1990).

²S. S. P. Parkin, N. More, and K. P. Roche, *Phys. Rev.*

Lett. **64**, 2304 (1990); J. Unguris, R. J. Celotta, and D. T. Pierce, *ibid.* **67**, 140 (1991); S. T. Purcell, W. Folkers, M. T. Johnson, N. W. E. McGee, K. Jager, J. aan de Stegge, W. B. Zeper, W. Hoving, and P. Grünberg, *ibid.* **67**, 903 (1991).

³R. E. Camley and J. Barnas, *Phys. Rev. Lett.* **63**, 664

- (1989).
- ⁴D. M. Edwards, J. Mathon, and R. B. Muniz, IEEE Trans. Magn. **MAG-27**, 3548 (1991).
- ⁵P. M. Levy, S. Zhang, and A. Fert, Phys. Rev. Lett. **65**, 1643 (1990); S. Zhang, P. M. Levy, and A. Fert, Phys. Rev. B **45**, 8689 (1992).
- ⁶J. Inoue, A. Oguri, and S. Maekawa, J. Phys. Soc. Jpn. **60**, 1149 (1991); J. Magn. Magn. Mater. **104-107**, 1883 (1992).
- ⁷A. Okiji, H. Nakanishi, K. Sakata, and H. Kasai, Jpn. J. Appl. Phys. **31**, L706 (1992).
- ⁸B. Velicky, Phys. Rev. **184**, 614 (1967).
- ⁹P. Soven, Phys. Rev. **156**, 809 (1969).
- ¹⁰H. Hasegawa, Phys. Rev. B **42**, 2368 (1990); **43**, 10 803 (1991); J. Phys. Condens. Matter **4**, 169 (1992).
- ¹¹P. M. Levy, K. Ounadjela, S. Zhang, Y. Wang, C. B. Sommers, and A. Fert, J. Appl. Phys. **67**, 5914 (1990).
- ¹²Besides the FM solution shown in Fig. 2(b), we obtained another FM solution in which an Fe moment at $n = 4$ is $-0.40\mu_B$. The latter solution was assumed to be less stable than the former and was discarded in the conductivity calculation.
- ¹³We assumed that $\Lambda_s^{\text{AFM}} = \Lambda_s^{\text{FM}}$ and $\Delta_s^{\text{AFM}} = \Delta_s^{\text{FM}}$ in the M_1 layer, while $\Lambda_s^{\text{AFM}} = \Lambda_{-s}^{\text{FM}}$ and $\Delta_s^{\text{AFM}} = \Delta_{-s}^{\text{FM}}$ in the M_2 layer, although coherent potentials generally depend on the configuration. This approximation is nearly satisfied in our numerical calculations for the Fe/Cr film (see Figs. 3 and 4).
- ¹⁴See, for a review, *Spin Fluctuations in Itinerant Electron Magnetism*, edited by T. Moriya (Springer, Berlin, 1985).
- ¹⁵H. Hasegawa, J. Phys. Soc. Jpn. **46**, 1504 (1979); **49**, 178 (1980).
- ¹⁶J. Hubbard, Phys. Rev. B **19**, 2626 (1979); **20**, 4584 (1979).
- ¹⁷H. Hasegawa, following paper, Phys. Rev. B **47**, 15 080 (1993).